A Full-waveform, Migration-based Deconvolution Approach to Locating Micro-seismic Events

J.B.U. Haldorsen (READ ASA), M. Milenkovic (READ ASA), N. Brooks (READ US), C. Crowell (READ US) & M.B. Farmani (READ ASA)*

Summary

We present a new approach to generating 3D location maps for micro-seismic events from 3-component data. The method combines full-waveform vector migration with an imaging condition based on semblance-weighted deconvolution. The semblance-weighted deconvolution keys in on the signal-to-noise conditions of the data to give a high-resolution, low-noise estimate of the locations for the micro-seimic sources. As the method requires no explicit time picking or event association, it is well suited to be run as an either fully-automated or a semi-automated process. Almost as a by-product, the method provides a natural measure of the uncertainty associated with the locations of the individual micro-earthquakes.

Submitted to the 74th EAGE Conference & Exhibition**, Copenhagen 2012**

Introduction

Tight rocks and shale reservoirs will often require active fracture treatments to stimulate flow. The need for information about the progress of this treatment, has led to a growing number of systems developed for monitoring the process. The most popular of these systems are designed to detect acoustics emissions generated by the breaking rock.

The stress in the rock is a combination of the stress introduced by the hydraulic-fracturing operation and the stress naturally present in the rock that is imposed by the environment. When this stress exceeds the elastic limit of the rock, the rock fails along lines of natural weakness, reopening pre-existing fractures, or generating new fractures related to intrinsic rock properties.

The fractures may be pulled open or they may allow the two sides to slip along the fracture plane. The fracture opening and possible slip will lead to the emission of a seismic signal that in turn may be recorded at receivers, deployed either on the surface or in adjacent boreholes.

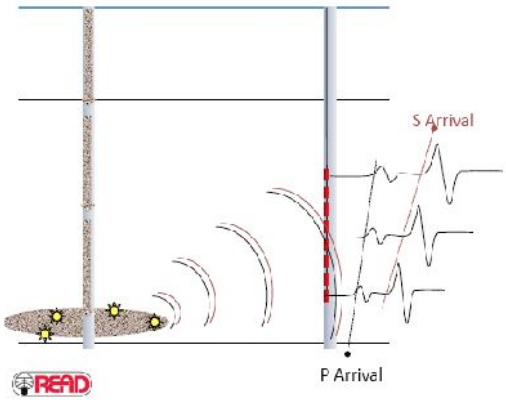

Figure 1 *Schematic view of the monitoring of the fracturing of a vertical well from a near-by vertical observation well.*

Micro-seismic ruptures

Figure 1 shows the schematics of the geometry for a monitoring system where the hydraulic activity in one well is monitored from a nearby observation well. The rupturing rock generates shear and compressional waves, which subsequently are recorded by an array of 3-component receivers in the observation well. The time-variation, or signature, of these wave fields carry information about the development of the rupture and the radiation pattern contains information about the spatial orientation and displacement of the fracture.

The polarization of the compressional and shear signals tells the direction of propagation of the wave-fields – i.e., these vectors will give the direction to the location of the rock rupture.

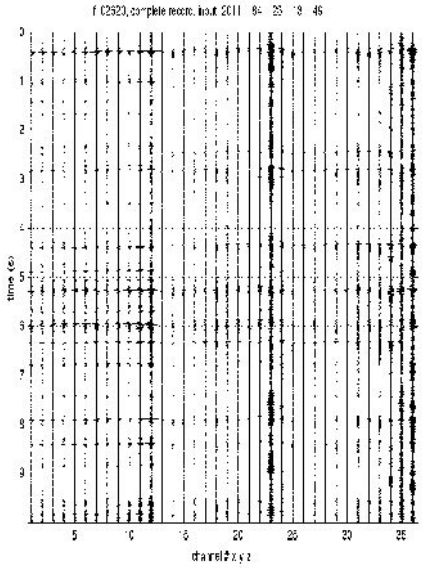

Figure 2 *a 10-s window of data recorded by a 12-level 3-component receiver array in an observation well near a well being a subject for hydraulic fracturing. In the display, the 12 vertical components are followed by 12 traces from each of the two horizontal components*

The location of the ruptures has conventionally been found in the reverse direction of the wave-field propagation by timing the compressional and shear arrivals. The distance from the observation point back to the rupture is given as the estimated time delay between the two wave-field components divided by the difference in their propagation slowness. The traditional methods for event location include identifying the separate arrivals and associating a shear wave arrival with the compressional signal.

.

Figure 2 shows a 10s window of data recorded by an array of 12 3-component receivers during a hydraulic fracturing operation. This window contains a large number of separate events of varying strength and varying degree of overlap. With an event frequency as high as this, it is difficult not only to associate shear and compressional arrivals, but also to pick consistent events across the array of

receivers. Any erroneous associations lead to miss-location of the hypocenters and/or unreasonably large uncertainties in their locations.

Migration

Surface and borehole-seismic data are widely used to generate images of rock formations. Conventionally, the data are first deconvolved in order to remove the source signature from the data. After deconvolving the data, the deconvolved data are used in a process commonly called migration to generate an image of the formation. The migration process generates the image by using the acoustic/elastic wave equation to relate travel times to acquisition geometry and formation properties.

With a rig source and a receiver array offset in a horizontal well several km from the rig, Haldorsen, et al. (2009) used the migration of converted shear and primary compressional wave fields to generate images of wave-field conversion points above and around the well. Similarly, Cheng, et al. (2010) used earthquake data to image conversion points along the Moho. What these two groups call a conversion point is where both wave fields are at the same place at the same time. In analyzing micro-earthquake data, this description would apply to the micro-seismic hypocenter.

When analyzing data generated by natural or induced micro-seismicity, one does not have the fortitude of knowing the signature of the source – rather, the acoustic signature of the microseism is one of the characteristics of the rupture one would like to estimate from the data.

Migration / Deconvolution

Extending this concept, and using the language of reverse-time migration (Chang and McMechan, 1986), we are suggesting that an array of 3-component receivers be used as a "transmission antenna", re-injecting the recorded wave field into the model of the formation. This will focus the wave fields, to give coherent, larger amplitudes at the voxel corresponding to the origin of the two wave fields, and incoherent, smaller amplitude at the other points in space (a "voxel" is the 3D equivalent of the 2D "pixel"). This process reconstructs the components of the recorded wave field that possibly could originate in any point in 3D space. For any point to be considered a hypocenter, the compressional (P) and shear (S) signatures will have to be both coherent and synchronous.

For a VTI medium, the polarization vector of the P wave field will stay in the same vertical plane (i.e., all ray-bending happens is vertical). The vertically and horizontally polarized components of the original shear wave field, S_h and S_v, will generally travel at different velocities, the S_v (vertical shear) staying mostly in the same vertical plane as the P polarization vector, the polarization of S_h, obviously horizontal. This is consistent with the observation that S and P generated by microseisms predominantly have polarization vectors in the same vertical plane. Subject to the properties of the noise in the data, this plane can be found by rotating the recorded data to minimize the energy on the horizontal component transverse to this plane. Mostly, this leaves only little coherent energy on the transverse axis. With the azimuth for the microseism established, the problem is reduced to 2D, greatly simplifying the computations, making a real-time, in-field interpretation of the data possible.

After identifying a candidate event n, one may select a reasonable-length data window centered at this event. As suggested by Haldorsen (2002), the first step in reconstructing the compressional signature $f^P_{nk}(\omega)$ for voxel k is to project the recorded data for receiver level j, $d_{jn}(\omega)$, onto the ray-vector p_{jk}, consistent with the geometry and the velocity model (ω denotes the angular frequency). The projected field is subsequently delayed by the appropriate travel times, t^P_{jk}. For the shear signal, $f^{Sv}_{nk}(\omega)$, the recorded signal is projected perpendicular to the emerging ray, then delayed and stacked:

$$f^P_{nk}(\omega) = \frac{1}{N_r}\sum_{j=1}^{N_r} \mathbf{p}^P_{jk} \bullet \mathbf{d}_{jn}(\omega)\, e^{-i\omega t^P_{jk}} \quad (1)$$

$$f^{Sv}_{nk}(\omega) = \frac{1}{N_r}\sum_{j=1}^{N_r} [\mathbf{p}^{Sv}_{jk} \times \mathbf{d}_{jn}(\omega)]_T\, e^{-i\omega t^{Sv}_{jk}} \quad (2)$$

To be a credible candidate for a microseism event, the P and S wave fields would have to have similar waveforms - and be synchronous. This "imaging condition" is measured by the deconvolution of the estimated P signature into the estimated S signature, using the deconvolution operator described by Haldorsen, et al. (1994), subsequently used by Haldorsen, et al. (2009) and Chen, et al. (2010). Their operator is designed to broaden the spectrum of the inverse of the estimated source signal at the same time as minimizing any additional energy left in the data. The deconvolved wave field becomes:

$$I_{nk}(\omega) = \frac{f^{P*}_{nk}(\omega) f^{Sv}_{nk}(\omega)}{E^{P}_{nk}(\omega)} \quad (3)$$

where $E^{P}_{nk}(\omega)$ is the frequency-by-frequency average energy of the compressional-projected wave field within the time-window event n

$$E^{P}_{nk}(\omega) = \frac{1}{N_r} \sum_{j=1}^{N_r} \left| \mathbf{p}^{P}_{jk} \bullet \mathbf{d}_{jn}(\omega) \right|^2 \quad (4)$$

If the shear wave field is both coherent and synchronous with the compressional wave field, the deconvolved shear will peak at t=0 with a resolution (or width of the peak) given by the bandwidth of "significant" coherent energy in the two wave fields. The image is thus formed at each image voxel by the value at t=0 of the deconvolved field.

Using appropriate velocity models, either pre-existing or ones generated from available sonic logs, one can speed up the calculations by pre-calculating the travel times and the ray-angles at the receivers for each voxel-receiver combination. As argued above, for a VTI medium, these calculations are further simplified and sped up by limiting them to a fixed-azimuth 2D plane.

Figure 3 shows a 0.35 s window of 3C data surrounding a possible micro-seismic event. Figure 4 shows the same data after rotation to minimize the transverse component. Figure 5 shows the image obtained from the rotated data, showing a clear and isolated peak at a depth of 2070 m and distance 272 m away from the receiver array (the azimuth was found by the data rotation giving Figure 4). The variance of the peak gives a direct measure of location uncertainty.

$I_{nk}(\omega)$ given by equation (3) has the form of a conventional correlation, where the cross-energy at a given frequency is weighted by the inverse of the average energy at this same frequency. Haldorsen, et al. (1994) shows that this process gives deconvolved data at the maximum bandwidth. They also show that this process is inherently stable and should require no additional frequency tinkering and should therefore be well suited for automatic processing.

In Figures 6 and 7, we show the compressional and shear wave fields estimated at the maximum of Figure 5. The time reference for both is relative to the beginning of the 10-s record. We can observe that two functions both have a maximum at around 0.35 s. Their synchronicity is

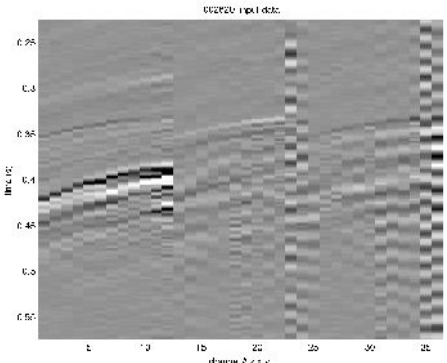

Figure 3 *A 0.35s section of the 10-s record in Figure 2, centered at around 0.4s on a possible S_v micro-seismic event. The display shows 12 receivers oriented vertically, followed by 12 oriented to the east and 12 to the north.*

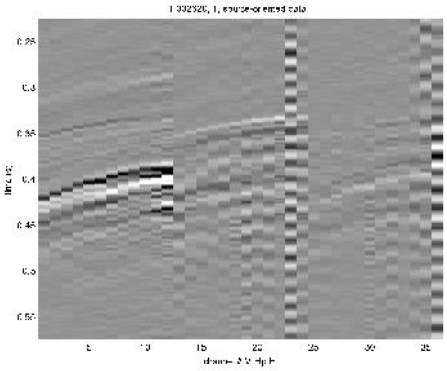

Figure 5 *The data from Figure 3 after minimizing the energy on the transverse (3^{rd}) components.*

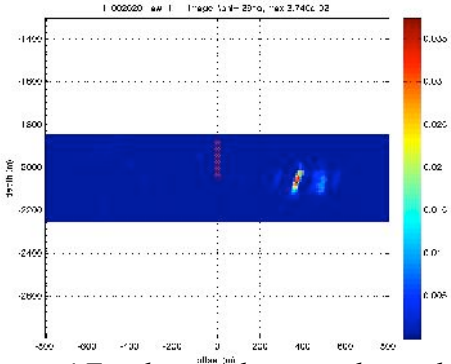

Figure 4 *Fixed-azimuth image obtained from the vertical and in-line (1^{st} and 2^{nd}) components from Figure 4.*

confirmed by the correlation function between the two functions shown in Figure 8a. The deconvolution of the same two functions, in Figure 8b, shows that the deconvolution gives a sharper peak with shorter duration (wider bandwidth) and surrounded by less noise artifacts.

The locations found by migration are consistent with results from using conventional method.

Conclusions

The combination of migration and deconvolution gives direct measurement of the locations of micro-seismic hypocenters with associated location uncertainties. The method requires no explicit time picking or event association and can therefore be run either fully or partly automatic.

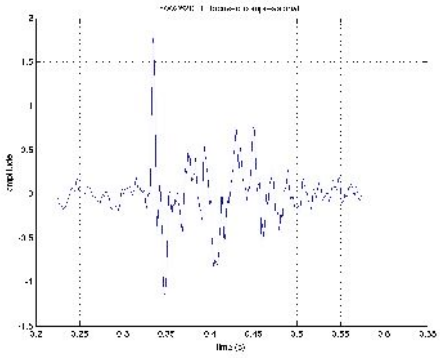

Figure 6 *The compressional field reconstructed from the data in Figure 4, at a depth of 2070 m and offset of 272 m at the azimuth of the image in Figure 5.*

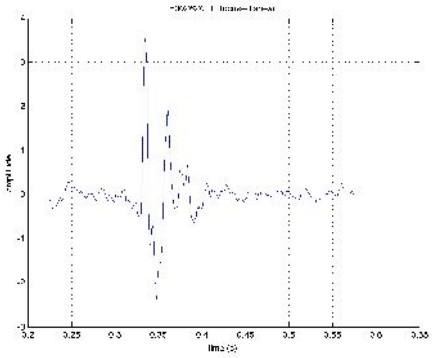

Figure 7 *The shear field reconstructed from the data in Figure 4, at a depth of 2070 m and offset of 272 m at the azimuth of the image in Figure 5.*

Acknowledgements

We would like to thank the Management in READ ASA for allowing us to publish the method and to an unnamed client for allowing us to use their data for testing the algorithms.

References

Chen, C.-W., D. E. Miller, H. A. Djikpesse, J. B. U. Haldorsen, and S. Rondenay, 2010, Array-conditioned deconvolution of multiple component teleseismic recording, Geophys. J. Int., 182, 967-976

Chang, W. F., and McMechan, G. A., 1986, Reverse-time migration of offset vertical seismic
profiling data using the excitation-time imaging condition: Geophysics, **51**, 67-84

Haldorsen, J. B. U., 2002. Converted-shear and compressional images using Projection Imaging. 64th EAGE Conference & Exhibition, Extended Abstracts, F031.

Haldorsen, J. B. U., W. S. Leaney, R. T. Coates, S. A. Petersen, H. I Rutledal, S. Hess, 2009, "Converted Wave Imaging Using VSP data: Looking up from an Extended-reach Horizontal Well", paper T034, 2009 EAGE Conference, Amsterdam

Haldorsen, J. B. U., Miller, D. E. and Walsh, J. J., 1994. Multichannel Wiener deconvolution of vertical seismic profiles. Geophysics, **59**, 1500-1511.

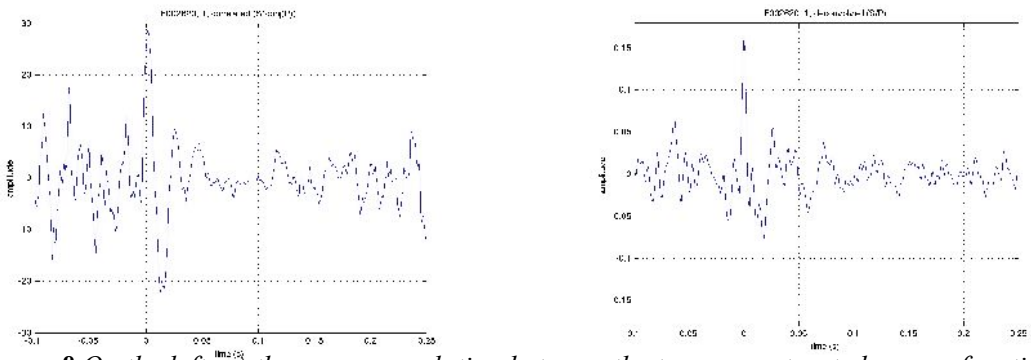

Figure 8 *On the left: a) the cross-correlation between the two reconstructed source functions shown in Figure 6 and 7. On the right: b) the deconvolution of the same two source functions.*